High-frequency conductivity and phonon properties of $La_{7/8}Sr_{1/8}MnO_3$

F. Mayr, C. Hartinger, M. Paraskevopoulos, A. Pimenov, J. Hemberger, and A. Loidl
Experimentalphysik V, Elektronische Korrelationen und Magnetismus, Institut für Physik, Universität Augsburg, D-86135 Augsburg, Germany

A. A. Mukhin
General Physics Institute of the Russian Academy of Sciences, 117942 Moscow, Russia

A. M. Balbashov
Moscow Power Engineering Institute, 105835 Moscow, Russia

(Received 15 July 1999; revised manuscript received 2 August 2000)

We report on broadband frequency-dependent conductivity experiments on $La_{7/8}Sr_{1/8}MnO_3$ that cover the frequency range from 0.3 meV (≈ 3 cm^{-1}) to 5 eV ($\approx 4\times10^4$ cm^{-1}). At all frequencies investigated, the temperature dependence of $\sigma'(\nu)$ reflects the structural and magnetic phase transitions. At low frequencies we find the typical characteristics of hopping conduction. The optical conductivity at frequencies above the phonon modes reveals strong changes at the structural and magnetic phase transitions and can best be described in terms of polaronic conduction. In addition, we carefully analyzed the temperature dependence of the phonon modes. Distinct anomalies in the eigenfrequencies and the appearance of side bands signal structural phase transitions.

I. INTRODUCTION

The doped perovskitelike manganites, which have been investigated in great detail in the 1950s,[1] again came into the focus of experimentalists and theoreticians, after colossal magneto-resistance effects were reported.[2] The complex phase diagram of $La_{1-x}Sr_xMnO_3$ at low doping levels[3] can only be explained assuming charge[4,5] and orbital order[3,6] of the manganese ions in addition to superexchange and double exchange (DE) interactions.[7]

It now seems to be experimentally established that close to $x=1/8$, the ground state is an insulating ferromagnet (FM), followed by a second magnetically ordered phase at elevated temperatures that most probably is a canted antiferromagnetic[3] (CA) or a mixed phase (on the basis of experiments published so far, an electronic phase separation in this temperature and concentration regime cannot be excluded). Also, a second ferromagnetic metallic phase has been claimed for this compound.[6] The CA phase evolves in the orthorhombic O' phase that reveals the orbital order[8] of pure $LaMnO_3$.

For the $La_{7/8}Sr_{1/8}MnO_3$ crystal under investigation, the following sequence of structural phase transitions was observed:[3] The transition at $T_{RO}=450$ K from rhombohedral to orthorhombic (O) is followed by a transition into a Jahn-Teller (JT) –distorted orthorhombic (O') ($T_{OO'}=270$ K) and finally by a transformation into an orthorhombic (O'') phase ($T_{O'O''}=140$ K) that probably reveals charge and orbital order.[3–6] A canted magnetic structure is established at $T_{CA}=180$ K, and a FM and insulating phase appears below 140 K.

Optical conductivity spectra have been reported for a variety of manganites[9–16] and it soon became clear that polaronic transport is of outstanding importance.[9–13] There has been one attempt to relate the infrared absorption in La:$CaMnO_3$ to the opening of a gap due to spin-density wave formation.[14] There are detailed theoretical predictions for optical conductivity due to polaronic transport.[17–19]

In pure $LaMnO_3$ with a long-range JT distortion, the e_g bands split into two subbands, separated by approximately 1.9 eV (Ref. 15). Of course, on-site d-d transitions are dipole forbidden. It is speculated that the lower subband hybridizes considerably with the oxygen $2p$ bands yielding finite dipolar transition matrix elements. A systematic study of low-doped $La_{1-x}Sr_xMnO_3$ has been performed by Okimoto *et al.*[16] on single crystals with strontium concentrations $x=0$, 0.1, 0.175, and 0.3. For $x=0.1$, with decreasing temperature they observed an increase of the midinfrared conductivity close to 0.5 eV that was interpreted to represent a typical polaron binding energy. This midinfrared peak in the conductivity has been qualitatively explained by Millis *et al.*[19] as an electronic transition from an occupied site (Mn^{3+}) to an adjacent occupied site (Mn^{3+}) or an unoccupied site (Mn^{4+}). A further investigation on polycrystalline samples with strontium concentrations $x=0.125$ has been reported by Jung *et al.*[20] These authors again observed an increase of the midinfrared conductivity close to 0.4 eV in addition to a broad interband transition at 1.6 eV. The midgap conductivity was explained in terms of small polarons, with an optical weight that strongly increases in the magnetically ordered phase as a consequence of the highly enhanced hopping probability in the FM state. However, in these investigations the optical conductivity never has been related to the complex structural phase diagram with the sequence of structural phase transitions with different orbital order, and this is one aim of the present study. In addition, we present detailed conductivity data in the broad frequency range from 3 cm^{-1} to 40 000 cm^{-1}.

The cubic ABO_3 perovskites display three main infrared (IR) bands located approximately at 180 cm^{-1}, 350 cm^{-1},

and 550 cm^{-1}. The 180-cm^{-1} mode results from an external vibration of the A ions against the BO_6 octahedra. The bending mode at 350 cm^{-1} arises from a simultaneous motion of the B and O ions in a certain direction against oxygen ions within a plane perpendicular to this direction. The bending mode is strongly affected by changes of the B-O-B bond angles. The high-frequency stretching mode corresponds to a motion of the B ions towards the oxygen ions and is sensitive to changes in the B-O bond lengths.

At room temperature the Raman and infrared phonons of rhombohedral $LaMnO_3$ were studied by Abrashev *et al.*[21] and were compared to the isostructural compound $LaAlO_3$. Fedorov *et al.*[22] studied the IR-active phonons in polycrystalline $LaMnO_3$ in the orthorhombic *Pnma* structure. Fourteen modes were identified. However, in most cases the fine structure of these modes could not be resolved. The temperature dependences of the internal phonon modes of ceramic $La_{0.7}Ca_{0.3}MnO_3$ were studied by Kim *et al.*[23] At room temperature, the three IR-active modes were detected at 165, 330, and 575 cm^{-1}. Below T_c and with decreasing temperatures, the high-frequency modes increased in frequency, while the external mode remained unshifted. A fine structure within these modes could not be observed. A single-crystal IR study has been performed by Boris *et al.*[24] and they were able to resolve a clear fine structure and a redistribution of oscillator strength within the bands. A rough overview concerning the temperature evolution of the phonon modes in $La_{7/8}Sr_{1/8}MnO_3$ has been given by Jung *et al.*[20] In the present paper, we study the temperature evolution of the eigenmode frequencies of the IR-active modes in detail, with special emphasis on possible changes at the structural and magnetic phase transitions.

II. EXPERIMENTAL DETAILS

Single crystals of $La_{7/8}Sr_{1/8}MnO_3$ were grown by the floating-zone method with radiation heating as described elsewhere.[25] The magnetic susceptibility and magnetization were measured using an Oxford ac susceptometer in fields up to 140 kOe. The magnetoresistance was measured in the same fields with a standard four-probe technique. Transmission experiments in a frequency range from 100 GHz (≈ 3 cm^{-1}) to 1 THz (≈ 30 cm^{-1}) were performed utilizing a set of backward-wave oscillators. These measurements were performed in a Mach-Zehnder configuration for measurements of transmission and phase shift, which allows a direct calculation of the real and imaginary part of the complex conductivity.[26]

In the IR regime, the temperature-dependent reflectivity has been measured using a Bruker IFS 113v Fourier transform (FT) -interferometer in the spectral range from 3 meV (≈ 25 cm^{-1}) to 0.5 eV (≈ 4000 cm^{-1}). For higher frequencies (0.25 eV–5 eV) a Bruker 66v/S FT spectrometer was used. The sample was placed in the exchange gas of a ^{4}He-bath cryostat, which was equipped with polypropylene windows for the far-infrared, KRS-5 windows for the midinfrared and near-infrared, and quartz windows for the VIS/uv range. The optical conductivity spectra were obtained by the Kramers-Kronig analysis of the reflectivity data. For this analysis, we used the room-temperature data of Jung *et al.*[20] for $x=0.125$ in the range from 5 eV up to 30 eV. For higher energies, a smooth ν^{-4} extrapolation to zero reflectivity was employed.

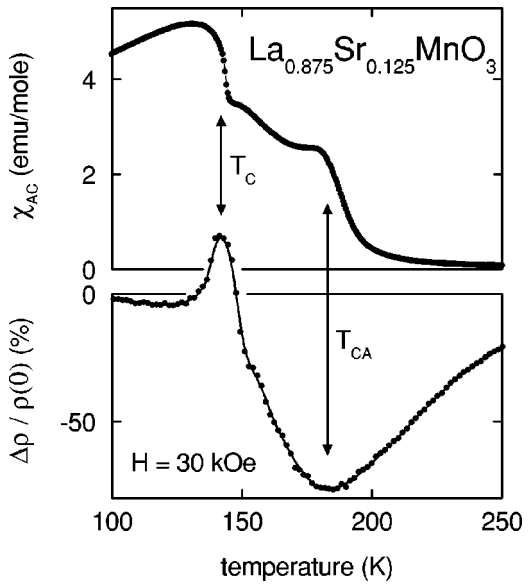

FIG. 1. Temperature dependence of the ac susceptibility χ_{AC} (upper frame) and the magnetoresistance $\Delta\rho/\rho(0)=[\rho(H)-\rho(0)]/\rho(0)$ in an external field of 30 kOe (lower frame) for $La_{7/8}Sr_{1/8}MnO_3$. The two magnetic transitions at T_{CA} and T_c are indicated by vertical arrows.

III. RESULTS AND DISCUSSION

To characterize the single crystal under investigation, we performed resistivity, susceptibility, and magnetization experiments. Figure 1 shows the susceptibility χ_{AC} (upper frame) and the magnetoresistance $[\rho(30\ kOe)-\rho(0\ kOe)]/\rho(0\ kOe)$ (lower frame) as function of temperature. Clearly, two magnetic transitions close to 180 K and 140 K can be identified. From the shape of the susceptibility curve, one would suspect that both transitions are strongly ferromagnetic in nature. It is interesting to note that at the upper transition, strong, negative magnetoresistance (MR) effects are revealed, while at the low-temperature transition, a significant, positive MR is observed. So the ground state is even more insulating than the intermediate phase. The lower transition also coincides with a structural phase transition that commonly is termed charge order transition.

To gain more insight into this complex phase diagram, Fig. 2 shows the magnetization and the magnetoresistance as a function of field: paramagnetism is detected in the orthorhombic O phase (295 K) and in the JT-distorted O' phase (200 K). At 170 K, a FM moment can be detected. The small antiferromagnetic hysteresis that shows up at low fields at 150 K, provides some evidence that this intermediate phase is a canted or a mixed phase. Finally, below 140 K, the full FM moment evolves, which becomes saturated at 10 K. A similar hysteresis can be detected in the MR at 150 K, and close to 140 K, a positive MR shows up (see also lower frame of Fig. 1).

From these investigations we conclude that the low-temperature state is a ferromagnetic insulator followed by a canted or mixed phase that is less insulating and reveals already a dominant FM component. A detailed phase diagram

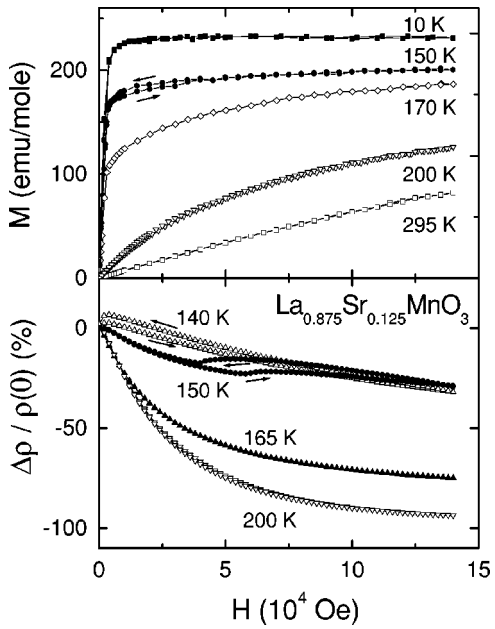

FIG. 2. Upper frame: Magnetization vs field as observed in $La_{7/8}Sr_{1/8}MnO_3$ at different temperatures. Lower frame: Isothermal magetoresistance $\Delta\rho/\rho(0)$ as function of external field.

has been published in Ref. 3, which is more complex than that recently derived by Xiong *et al.*,[27] at least concerning the magnetic phases.

Figure 3 shows the real and imaginary part of the dielectric permittivity $\epsilon^* = i\sigma^*/(\epsilon_0\omega)$ for wave numbers ranging from approximately 3 cm^{-1} (0.3 meV) to 4×10^4 cm^{-1} (5 eV) at different temperatures. Here, the room-temperature conductivity results correspond to the paramagnetic non-JT-distorted O phase, while the low-temperature results were taken in the ferromagnetic O'' phase. The dielectric constant is moderately temperature dependent at all frequencies, even

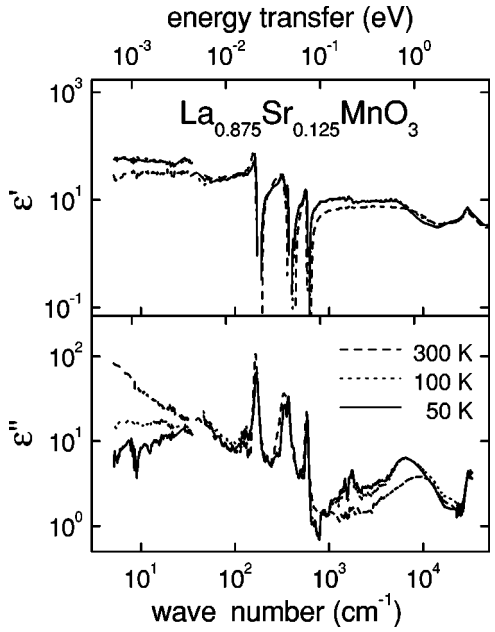

FIG. 3. Frequency dependence of the dielectric constant ϵ' (upper panel) and the dielectric loss ϵ'' (lower panel) in $La_{7/8}Sr_{1/8}MnO_3$ at 50 K (solid line), 100 K (dotted line), and 300 K (dashed line).

up to the visible frequency regime. Three different regimes, the subphonon regime, the phonon modes, and the regime of interband transitions, are clearly visible. For frequencies below the phonon modes, the dielectric constant is dominated by a large static value that amounts to approximately 60 at low temperatures and decreases to a value close to $\epsilon' = 30$ at room temperature. The origin of the small step in the frequency dependence of the dielectric constant close to 5 meV at low temperatures remains unexplained. It may be due to the strong increase of the magnetic permeability in the ferromagnetic low-temperature phase. In the vibrational frequency regime, via ionic polarizability, the dielectric constant is reduced to values close to 10 and is further reduced due to an interband transition close to 1 eV.

The dielectric loss at low frequencies is dominated by hopping processes of charge carriers strongly coupled to the lattice that are thermally excited, resulting in a strong temperature and frequency dependence. The importance of hopping conduction in low-doped $La_{1-x}Sr_xMnO_3$ was recently demonstrated by low-frequency measurements of the complex ac conductivity.[28] Above the phonon modes, we detect a strong transfer of spectral weight to lower frequencies when the ferromagnetic O'' phase is reached, which will be discussed later in detail. In the phonon regime, a strong, sublinear decrease ($\epsilon'' \sim \nu^{-0.75}$) of the dielectric background loss is observed, roughly independent of temperature. At room temperature this sublinear decrease extends to lower frequencies. This unusual feature can be explained neither in terms of ac hopping conductivity nor as dc contribution. This feature remains unchanged as a function of temperature for frequencies between 30 cm^{-1} and 100 cm^{-1}. The strong temperature dependence sets in well below the phonon modes, for energies <5 meV, and this clearly is the regime of hopping conductivity of localized charge carriers. At 50 K, $\epsilon''(\nu)$ increases indicating an increase of the conductivity $\sigma' \propto \omega\epsilon''$ with a frequency exponent larger than 1, not predicted by hopping models. Much more experimental work will be necessary to explore the dielectric properties in this low-frequency regime.

A. Phonon spectra

At the zone center, the cubic perovskites exhibit four fundamental optical and internal vibrations, three of which are infrared active.[29] In its orthorhombic structures $La{:}SrMnO_3$ is expected to reveal 25 IR-active modes.[30] A representative comparison of the phonon modes as observed in $LaMnO_3$ and $La_{7/8}Sr_{1/8}MnO_3$ at 250 K is shown in Fig. 4. Here, we plotted the real part of the optical conductivity σ' vs the photon wave number (100 $cm^{-1} \approx 3$ THz). At this temperature, both compounds reveal the JT-distorted O' phase. Nevertheless, the spectra look quite different. While more than 10 modes can be detected in the pure compound, only three bands can be identified for the doped crystal. Obviously weaker modes disappear or are smeared out due to disorder-induced broadening in the mixed crystal.

In the orthorhombic *Pnma* phase of pure $LaMnO_3$ 25 IR-active phonon modes have been predicted by lattice dynamic calculations by Smirnova.[30] Approximately 11 bands can be identified in Fig. 4 as indicated by arrows. The eigenfrequencies of these modes are located at the following wave num-

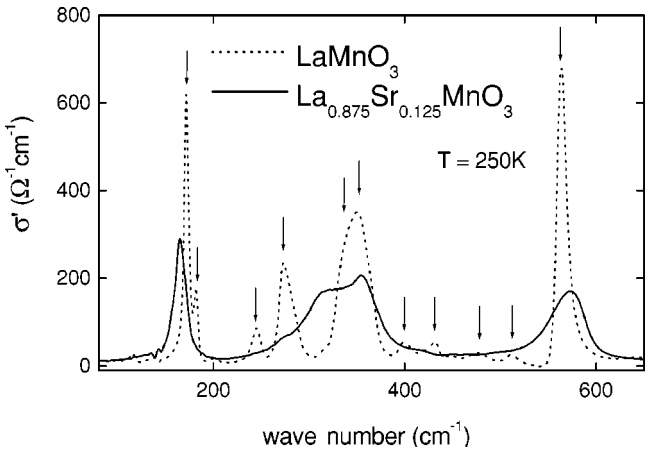

FIG. 4. Phonon modes as observed in $LaMnO_3$ (dashed line) and $La_{7/8}Sr_{1/8}MnO_3$ (solid line) by IR techniques at 250 K. At this temperature, both compounds reveal the JT-distorted O' phase. Oscillator eigenfrequencies that can be observed experimentally in $LaMnO_3$ are indicated by arrows.

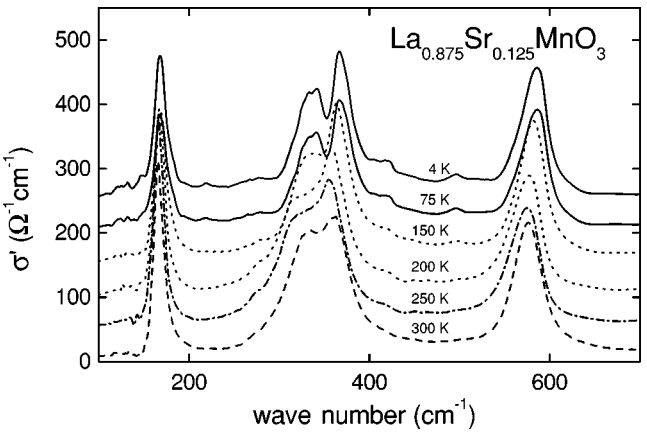

FIG. 5. Phonon modes in $La_{7/8}Sr_{1/8}MnO_3$ vs wave number at different temperatures [dashed line, 300 K (O/PM); dash-dotted line, 250 K (O'/PM); dotted lines, 200 K and 150 K (O'/CA); solid lines, 75 K and 4 K (O''/FM)]. For better clarity, the conductivity values have been shifted by 50 $\Omega^{-1}\,cm^{-1}$ for each temperature, except for the 300-K curve.

bers: 171, 181, 244, 273, 335, 352, 399, 431, 477, 512, and 563 cm^{-1} and can be compared with the theoretical predictions of phonon modes at 167, 186, 244, 264, 330, 367, (394/399), 506, and (560/562/579) cm^{-1} (Ref. 30). Here, the wave numbers in brackets indicate groups of vibrational modes that cannot be separated under the given experimental conditions (broadening due to sample inhomogeneities). Six modes at low frequencies (below 135 cm^{-1}) could not be observed experimentally, as well as a group located at (202/207/225) cm^{-1}, at (300/306/308) cm^{-1}, and at 599 cm^{-1}. Probably these modes are too weak in intensity to be observed above the experimental background. Astonishingly, the weak modes that we do observe close to 420 and 490 cm^{-1} are not predicted theoretically.

An IR study of polycrystalline powders has been presented by Fedorov *et al.*,[22] including a model calculation of IR-active modes. There exists severe disagreement between the two lattice-dynamic calculations of Smirnova[30] and Fedorov *et al.*[22] Experimentally, the latter authors observe a rather broad hump of optical density between 300 cm^{-1} and 500 cm^{-1}, but it is not straightforward to compare the optical density, which is the logarithm of the inverse transmittance, with the real part of the conductivity. In the lattice-dynamics calculation, they predict IR-active modes to appear at 443 cm^{-1} and 495 cm^{-1}. However, the intensity of these modes was predicted to be rather strong, not in agreement with our results. Clearly, further experimental and theoretical work is needed to explain these severe discrepancies between experimental observation and theoretical prediction.

In the Sr-doped compound, the splitting of the modes seems to be considerably reduced, and roughly three phonon groups can be detected in good agreement with previous reports.[21,23] For example, it seems that the three bands located between 250 and 380 cm^{-1} in the pure compound correspond to one smeared-out group between 280 and 300 cm^{-1} in $La_{7/8}Sr_{1/8}MnO_3$. This certainly is the result of a strongly reduced Jahn-Teller splitting. For a detailed comparison, lattice-dynamic calculations yielding eigenfrequencies and intensities are very important. Neutron-scattering studies have been performed by Reichardt and Braden;[31] however, they presented the phonon modes in the rhombohedral phases only. Similar studies in the JT-distorted O' phase are highly desirable.

The three orthorhombic phases O, O' and O'', which were detected as a function of temperature in $La_{7/8}Sr_{1/8}MnO_3$, are characterized by considerably different bond angles and different bond lengths,[32–34] and hence, some of the eigenfrequencies characteristic for these phases are expected to differ noticeably. Figure 5 shows the phonon modes in $La_{7/8}Sr_{1/8}MnO_3$ at some characteristic temperatures. As mentioned above, three phonon groups can be detected in agreement with what is expected in cubic perovskites. The band at intermediate frequencies (*bending*) is split, revealing most significant deviations from cubic symmetry due to the orthorhombic distortions. Both the bending and the high-frequency stretching modes reveal small shifts on decreasing temperature. In the three different structural phases (O, JT-distorted O', and O'') the splitting and shift of these modes should depend on the changes of the bond lengths at the structural phase transitions. The JT-distorted O' phase is characterized by two nonequivalent oxygen sites with nonequivalent Mn-O bond lengths. The difference of these bond lengths is most significant in the long-range Jahn-Teller–distorted O' phase and is almost zero in the O and O'' phases.[33] But astonishingly, apart from some minor changes, the overall spectra look rather similar at all temperatures (Fig. 5). Small side bands evolve at low temperatures. Most noticeable among these are small peaks located at 125, 220, and 500 cm^{-1}. Probably they indicate new zone-center modes in a superstructure due to charge or orbital order. Detailed lattice-dynamic calculations are necessary to clarify these questions.

Already a rough inspection of Fig. 5 shows that the frequency of the low-frequency mode, which is an external vibration, reveals a weak temperature dependence only. In contrast, the bending mode and the stretching mode show temperature dependences exceeding the experimental uncertainties that will be investigated in the following. The conductivity spectra at all temperatures were fitted assuming Lorentzian oscillators with oscillator strengths S_i, eigenfre-

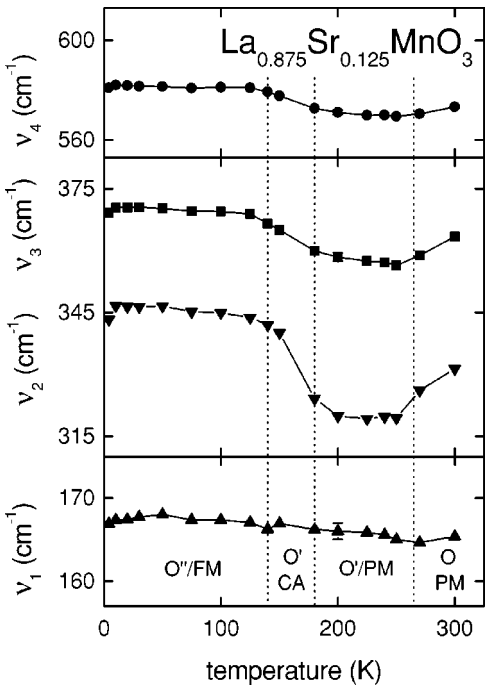

FIG. 6. Temperature dependences of the mode eigenfrequencies ν_i of the most significant modes in $La_{7/8}Sr_{1/8}MnO_3$. The phase-transition temperatures are indicated by vertical dashed lines. The lines are drawn to guide the eye.

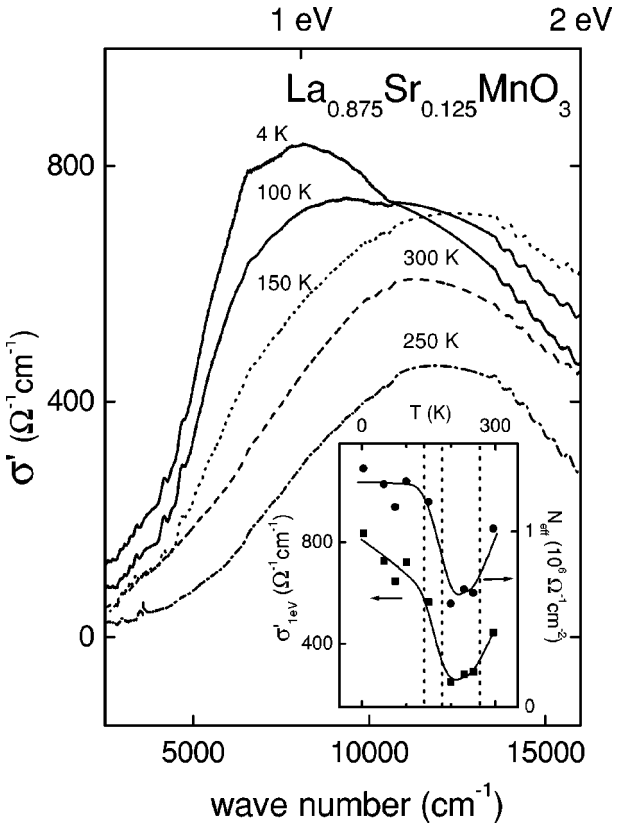

FIG. 7. Optical conductivity vs frequency in $La_{7/8}Sr_{1/8}MnO_3$ at different temperatures between 300 K and 4 K [300 K (dashed line), O/PM; 250 K (dash-dotted line), O'/PM; 150 K (dotted line), O'/CA; 100 K and 4 K (solid lines), O''/FM]. The inset shows the temperature dependence of the optical conductivity σ' as measured at 1 eV (left scale) and of the optical weight N_{eff} up to frequencies of 2 eV (right scale). The vertical dashed lines indicate the same phase-transition temperatures as in Fig. 6. The solid lines in the inset are drawn to guide the eye.

quencies ν_i, and damping constants γ_i. The limited resolution due to sample inhomogeneities and disorder hamper an exact analysis of eigenfrequencies, width, and oscillator strength; as in most cases these properties are highly correlated and the peaks cannot be separated exactly. For example, four IR-active modes hide below the stretching mode close to 580 cm^{-1} in the orthorhombic structure.[30] Hence, at the present stage of the work, and without theoretical predictions about symmetry-related splitting of the modes in the different structural phases, we only show the temperature dependence of the eigenfrequencies of the four most significant modes that have been fitted using one Lorentzian per peak. The result of this analysis is shown in Fig. 6. The temperatures of the structural and magnetic phase transitions are indicated as dotted lines. It immediately becomes clear that the frequency of the internal mode ($\nu_1 \approx 165$ cm^{-1}) only slightly increases on decreasing temperature as usually observed in anharmonic crystals. At the phase boundaries no anomalies can be detected within the experimental uncertainty. Weak but significant anomalies at the phase boundaries can be detected in the stretching mode ($\nu_4 \approx 565$ cm^{-1}) and in the high-frequency bending mode ($\nu_3 \approx 370$ cm^{-1}). Stronger anomalies, of the order of 10%, show up in the lower bending mode ($\nu_2 \approx 330$ cm^{-1}). In all cases but the internal mode, the eigenfrequencies slightly soften at the structural transition from the orthorhombic O to the Jahn-Teller–distorted orthorhombic O' structure. A strong increase appears at the magnetic phase boundary within the O' phase. It is unclear if this increase of the eigenfrequencies is due to the onset of magnetic order or is a precursor phenomenon of the charge and orbitally ordered O'' phase. An increase of the eigenfrequencies has been predicted by Lee and Min[35] when FM order is established in double-exchange materials. However, we would like to point out that in the $La_{7/8}Sr_{1/8}MnO_3$ sample under investigation, a FM and insulating ground state is reached below 140 K. And certainly DE cannot explain the appearance of this phase. We believe that the main effect of the phonon shifts results from a softening of the bending and stretching modes in the JT-distorted phase.

B. Optical conductivity

Figure 7 shows the frequency-dependent optical conductivity for various characteristic temperatures. At 300 K, the conductivity exhibits a broad peak close to 1.5 eV. We would like to recall that at 300 K, $La_{7/8}Sr_{1/8}MnO_3$ reveals the non-JT–distorted O phase. This peak is only slightly reduced when entering into the Jahn-Teller–distorted O' phase but still appears at the same frequency. It is the common belief that this feature either indicates an interband transition between the JT-split e_g modes or an intersite transition between neighboring Mn^{3+} and Mn^{4+} ions.[19] The former case is rather unlikely as this transition is dipole forbidden. It could be allowed via disorder effects or via a hybridization of the oxygen p levels with the Mn d states. It is also unclear why the conductivity is so similar in the O and O' phases. The

most probable explanation lies in the existence of dynamic JT distortions at 300 K, which, at the time scale of this optic investigation, appear to be almost static. And indeed, local JT distortions were detected in pulsed neutron-diffraction experiments, which persist even up to Sr concentrations $x \approx 0.4$.[36] That indeed the structural phase transitions between O, O', and O'' locally preserve the JT distortions has been demonstrated by Xiong *et al.*[27] who showed that at these phase transitions only the fraction of coherent (cooperative) to incoherent distortions is changed.

In the ferromagnetic O'' phase, the spectral weight is shifted to lower frequencies, and a rather asymmetric peak appears close to 1 eV at the lowest temperatures. The inset of Fig. 7 compares the temperature dependence of the conductivity as measured at 1 eV to the total optical weight N_{eff} up to frequencies of 2 eV. N_{eff} is a direct measure of the kinetic energy of mobile charge carriers. The temperature dependence of the conductivity at 1 eV as well as of N_{eff} reveal significant anomalies at the structural and magnetic phase boundaries (shown as dotted lines). Obviously, N_{eff} below 2 eV is completely dominated by polaronic effects, and polaronic transport is strongly enhanced in the O''/FM/I phase. σ'(1 eV) and N_{eff} reveal almost the same temperature dependence as observed for the eigenfrequencies of the vibrational modes (Fig. 6). This indeed indicates a strong coupling of the electronic and phonon properties, and certainly points towards a polaronic origin of the conductivity peak close to 1 eV.

The experimental findings of Fig. 7 only qualitatively resemble the model calculations of Millis *et al.*[19] The results of Fig. 7 indicate a system characterized by a rather strong electron-phonon coupling, with large frozen-in lattice distortions even at $T=0$ K. In the model calculations, the peak in σ' shifts to lower frequencies and grows in intensity at the ferromagnetic phase transition. However, we have to keep in mind that in $La_{1-x}Sr_xMnO_3$ ($x=1/8$) the ground state is a ferromagnetic insulator characterized by charge order and probably by a new type of orbital order. We believe that the conductivity at low temperatures is due to a polaronic excitation within the O'' phase with a different binding energy.

IV. CONCLUSIONS

We studied in detail the phonon spectra and the optical conductivity in $La_{7/8}Sr_{1/8}MnO_3$ as a function of temperature. We paid special attention to the structural and magnetic phase transitions of the system where the phonon spectra show significant anomalies in the bending and stretching modes, being detected in the eigenfrequencies.

From the frequency and temperature dependence of the optical conductivity at low frequencies, we conclude that in $La_{7/8}Sr_{1/8}MnO_3$ the conductivity is dominated by hopping processes of localized charge carriers, and that below room temperature, no Drude peak can be observed.

In the O and O'' phases, the optical conductivity shows the signature of small polarons. The experimental results seem to be well described by the model of Millis *et al.*[19] who calculated the theoretical conductivity of charge carriers coupled to phonons and to ferromagnetically aligned core spins. For $La_{7/8}Sr_{1/8}MnO_3$, the electron-phonon coupling is strong enough to localize these polarons. From an experimental point of view, it now seems important to investigate the melting of these polarons and the formation of a Fermi liquid at the metal-to-insulator transition close to $x=0.17$.

ACKNOWLEDGMENTS

This work was partly supported by the BMBF under Contract No. 13N6917/Elektronische Korrelationen und Magnetismus, by the Sonderforschungsbereich 484 from the Deutsche Forschungsgemeinschaft, and by the European Community via INTAS 30850.

[1] G.H. Jonker and J.H. van Santen, Physica (Amsterdam) **16**, 337 (1950); E.O. Wollan and W.C. Koehler, Phys. Rev. **100**, 545 (1955).

[2] R. von Helmolt, J. Wecker, B. Holzapfel, L. Schultz, and K. Samwer, Phys. Rev. Lett. **71**, 2331 (1993); K. Chahara, T. Ohno, M. Kasai, Y. Kanke, and Y. Kozono, Appl. Phys. Lett. **62**, 780 (1993); S. Jin, T.H. Tiefel, M. McCormack, R.A. Fastnacht, R. Ramesh, and L.H. Chen, Science **264**, 413 (1994).

[3] M. Paraskevopoulos, F. Mayr, C. Hartinger, A. Pimenov, J. Hemberger, P. Lunkenheimer, A. Loidl, A.A. Mukhin, V.Yu. Ivanov, and A.M. Balbashov, J. Magn. Magn. Mater. **211**, 118 (2000); M. Paraskevopoulos, F. Mayr, J. Hemberger, A. Loidl, R. Heichele, D. Maurer, V. Müller, A.A. Mukhin, and A.M. Balbashov, J. Phys.: Condens. Matter **12**, 3993 (2000).

[4] H. Kawano, R. Kajimoto, M. Kubota, and H. Yoshizawa, Phys. Rev. B **53**, R14 709 (1996).

[5] Y. Yamada, O. Hino, S. Nohdo, R. Kanao, T. Inami, and S. Katano, Phys. Rev. Lett. **77**, 904 (1996).

[6] Y. Endoh, K. Hirota, S. Ishihara, S. Okamoto, Y. Murakami, A. Nishizawa, T. Fukuda, H. Kimura, H. Nojiri, K. Kaneko, and S. Maekawa, Phys. Rev. Lett. **82**, 4328 (1999).

[7] C. Zener, Phys. Rev. **82**, 403 (1951).

[8] Y. Murakami, J.P. Hill, D. Gibbs, M. Blume, I. Koyama, M. Tanaka, H. Kawata, T. Arima, Y. Tokura, K. Hirota, and Y. Endoh, Phys. Rev. Lett. **81**, 582 (1998).

[9] K.H. Kim, J.H. Jung, D.J. Eom, T.W. Noh, J. Yu, and E.J. Choi, Phys. Rev. Lett. **81**, 4983 (1998).

[10] Y. Okimoto, Y. Tomioka, Y. Onose, Y. Otsuka, and Y. Tokura, Phys. Rev. B **59**, 7401 (1999).

[11] Y. Moritomo, A. Machida, K. Matsuda, M. Ichida, and A. Nakamura, Phys. Rev. B **56**, 5088 (1997).

[12] A. Machida, Y. Moritomo, and A. Nakamura, Phys. Rev. B **58**, R4281 (1998).

[13] S.G. Kaplan, M. Quijada, H.D. Drew, D.B. Tanner, G.C. Xiong, R. Ramesh, C. Kwon, and T. Venkatesan, Phys. Rev. Lett. **77**, 2081 (1996).

[14] P. Calvani, G. De Marzi, P. Dore, S. Lupi, P. Maselli, F. D'Amore, S. Gagliardi, and S-W. Cheong, Phys. Rev. Lett. **81**, 4504 (1998).

[15] J.H. Jung, K.H. Kim, D.J. Eom, T.W. Noh, E.J. Choi, J. Yu, Y.S. Kwon, and Y. Chung, Phys. Rev. B **55**, 15 489 (1997).

[16] Y. Okimoto, T. Katsufuji, T. Ishikawa, T. Arima, and Y. Tokura,

Phys. Rev. B **55**, 4206 (1997); Y. Okimoto, T. Katsufuji, T. Ishikawa, A. Urushibara, T. Arima, and Y. Tokura, Phys. Rev. Lett. **75**, 109 (1995).
[17] D. Emin, Phys. Rev. B **48**, 13 691 (1993).
[18] A.S. Alexandrov and A.M. Bratkovsky, cond-mat/9901340 (unpublished).
[19] A.J. Millis, R. Mueller, and B.I. Shraiman, Phys. Rev. B **54**, 5389 (1996); **54**, 5405 (1996).
[20] J.H. Jung, K.H. Kim, H.J. Lee, J.S. Ahn, N.J. Hur, T.W. Noh, M.S. Kim, and J.-G. Park, Phys. Rev. B **59**, 3793 (1999).
[21] M.V. Abrashev, A.P. Litvinchuk, M.N. Iliev, R.L. Meng, V.N. Popov, V.G. Ivanov, R.A. Chakalov, and C. Thomsen, Phys. Rev. B **59**, 4146 (1999).
[22] I. Fedorov, J. Lorenzana, P. Dore, G. De Marzi, P. Maselli, P. Calvani, S.-W. Cheong, S. Koval, and R. Migoni, Phys. Rev. B **60**, 11 875 (1999).
[23] K.H. Kim, J.Y. Gu, H.S. Choi, G.W. Park, and T.W. Noh, Phys. Rev. Lett. **77**, 1877 (1996).
[24] A.V. Boris, N.N. Kovaleva, A.V. Bazhenov, P.J.M. van Bentum, Th. Rasing, S-W. Cheong, A.V. Samoilov, and N.-C. Yeh, Phys. Rev. B **59**, R697 (1999).
[25] A.M. Balbashov, S.G. Karabashev, Ya.M. Mukovskiy, and S.A. Zverkov, J. Cryst. Growth **167**, 365 (1996).
[26] A.A. Volkov, Yu.G. Goncharov, G.V. Kozlov, S.P. Lebedev, and A.M. Prokhorov, Infrared Phys. **25**, 369 (1985); A.A. Volkov, G.V. Kozlov, S.P. Lebedev, and A.M. Prokhorov, *ibid.* **29**, 747 (1989).
[27] X. Xiong, B. Dabrowski, O. Chmaissem, Z. Bukowski, S. Kolesnik, R. Dybzinski, C.W. Kimball, and J.D. Jorgensen, Phys. Rev. B **60**, 10 186 (1999).
[28] A. Seeger, P. Lunkenheimer, J. Hemberger, A.A. Mukhin, V.Yu. Ivanov, A.M. Balbashov, and A. Loidl, J. Phys.: Condens. Matter **11**, 3273 (1999).
[29] W.G. Fateley, N.T. McDevitt, and F.F. Bentley, Appl. Spectrosc. **25**, 155 (1971).
[30] I.S. Smirnova, Physica B **262**, 247 (1999).
[31] W. Reichardt and M. Braden, Physica B **263-264**, 416 (1999).
[32] A.K. Bogush, V.I. Pavlov, and L.V. Balyko, Cryst. Res. Technol. **18**, 589 (1983).
[33] L. Pinsard, J. Rodríguez-Carvajal, A.H. Moudden, A. Anane, A. Revcolevschi, and C. Dupas, Physica B **234–236**, 856 (1997); L. Pinsard, J. Rodríguez-Carvajal, and A. Revcolevschi, J. Alloys Compd. **262-263**, 152 (1997).
[34] D.N. Argyriou, J.F. Mitchell, C.D. Potter, D.G. Hinks, J.D. Jorgensen, and S.D. Bader, Phys. Rev. Lett. **76**, 3826 (1996).
[35] J.D. Lee and B.I. Min, Phys. Rev. B **55**, 12 454 (1997).
[36] D. Louca, T. Egami, E.L. Brosha, H. Röder, and A.R. Bishop, Phys. Rev. B **56**, R8475 (1997).